Nonlinear standing wave excitation in very-high-frequency capacitive discharges

Kai Zhao, De-Qi Wen, Yong-Xin Liu, You-Nian Wang*

kaizhao@dlut.edu.cn, yxliu129@dlut.edu.cn, ynwang@dlut.edu.cn

Plasma Simulations and Experiments Group (PSEG)
School of Physics, Dalian University of Technology, China

International Online Plasma Seminar
16 July 2020

Agenda

- ***Nonlinear standing wave excitation in a single-frequency CCP***
- ***Suppressing nonlinear standing wave excitation via the EAE***
- ***Role of the low-frequency source on the nonlinear standing wave excitation in a dual-frequency CCP***
- ***Summary***

1 Nonlinear standing wave excitation in a single-frequency CCP

1.1 Introduction: applications of CCP sources

- Capacitively coupled plasmas (CCPs) have been widely employed in etching and thin film deposition processes in the semiconductor industries.

No	Process	Image	Equipment Structure	No	Process	Image	Equipment Structure
①	Oxidation	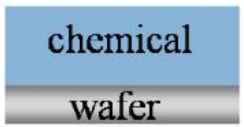	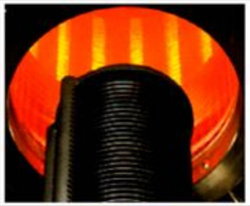	⑤	Ion-Implantation	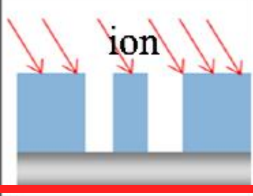	
②	Lithography	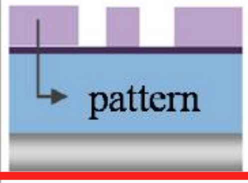	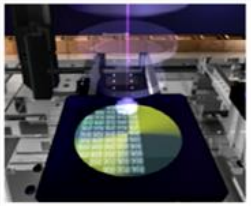	⑥	Chemical Vapor Deposition	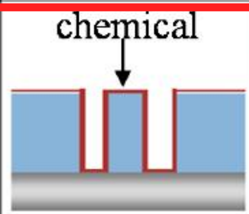	
③	Etching	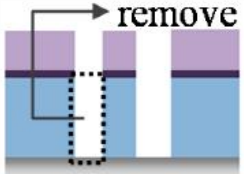	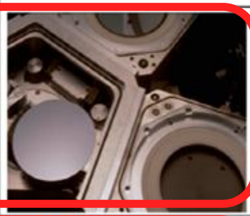	⑦	Metal Deposition	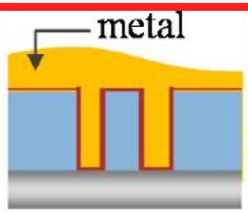	
④	Strip & Cleaning	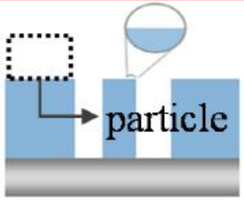		⑧	Chemical and Mechanical Planarization		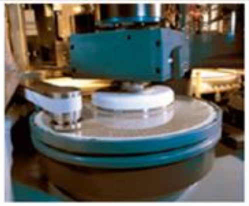

1.1 Introduction: current trends

➢ **Trend-1: increase of frequency**

Higher excitation frequencies produce *reduced ion bombarding energy*, required to minimize the substrate damage.

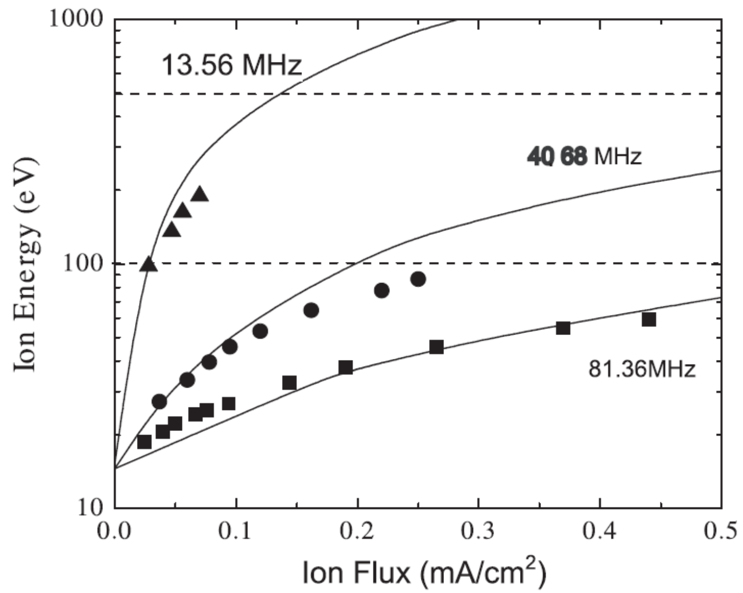

➢ **Trend-2: increase of reactor size**

Larger plasma reactors are required *as wafer size increases*, in order to improve the throughput.

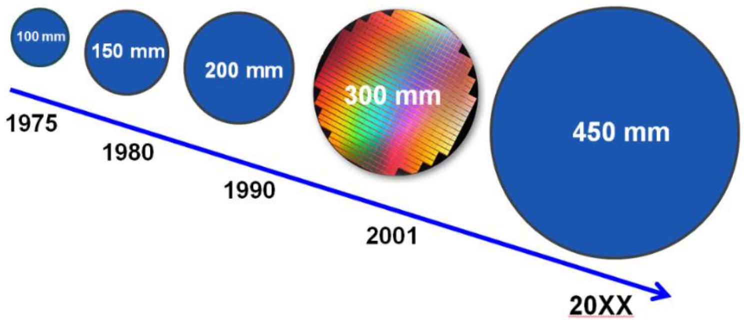

1.1 Introduction: standing wave effect

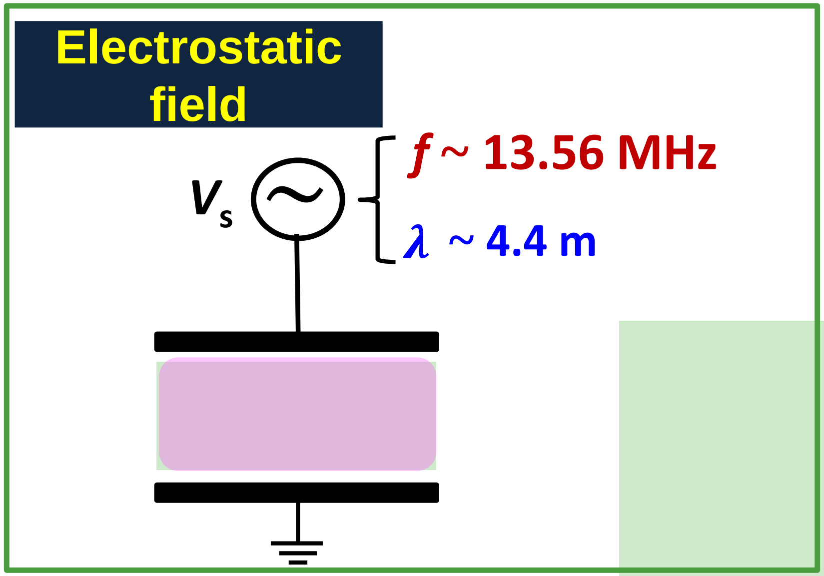

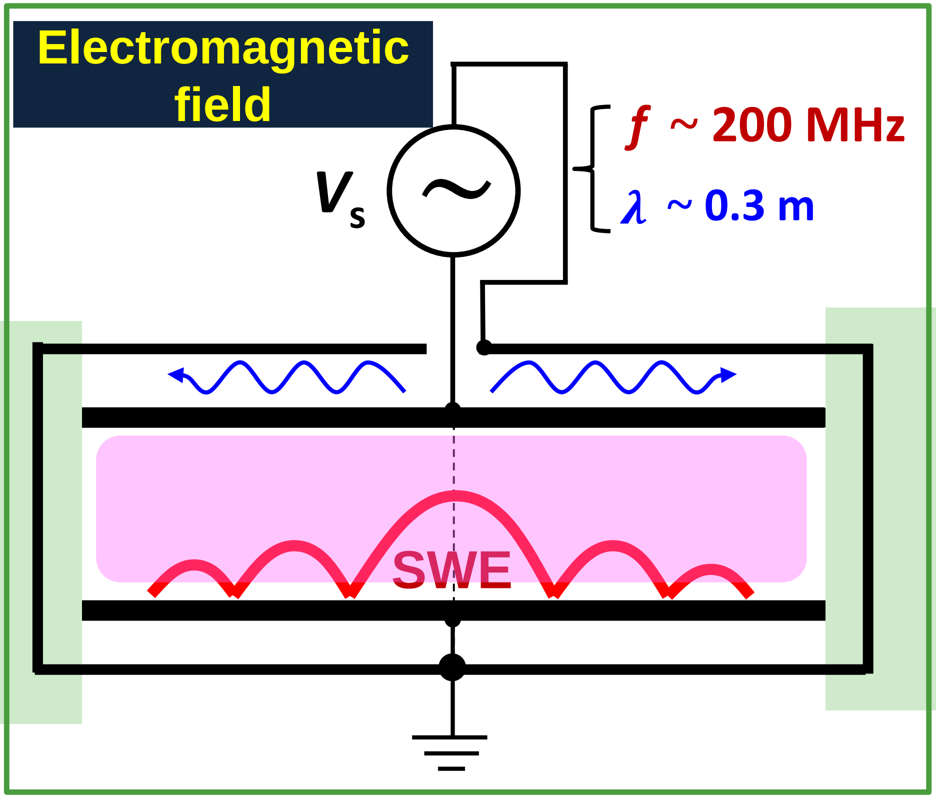

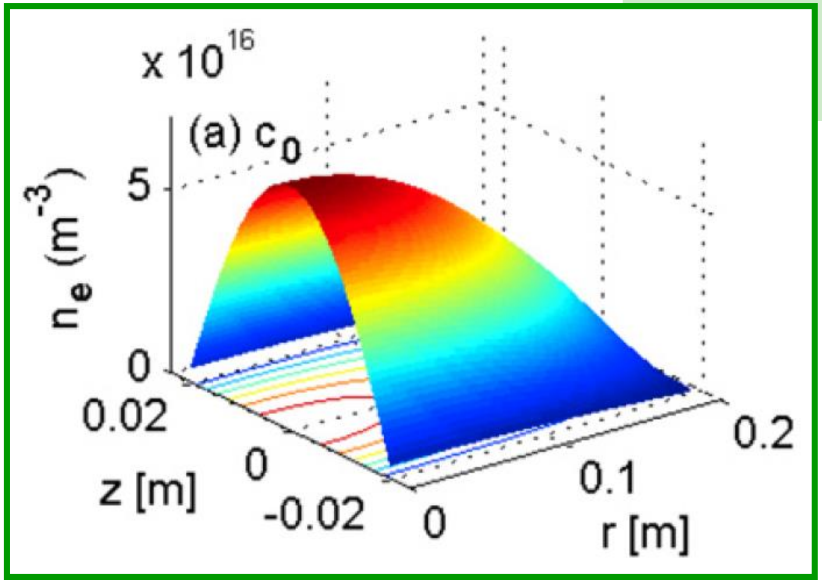

Causing a severe plasma non-uniformity!

1.1 Introduction: causes of plasma nonuniformity

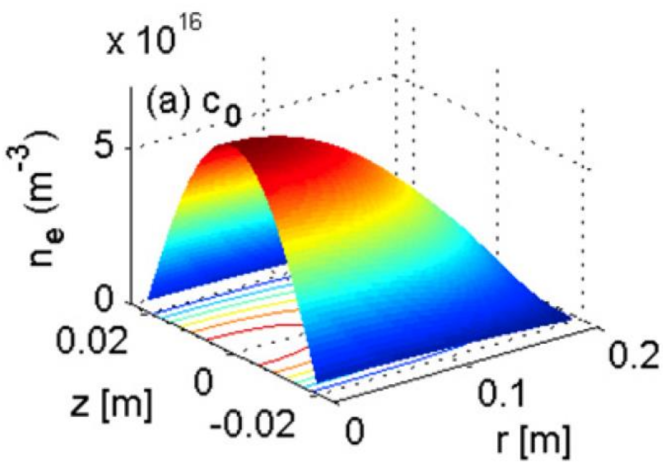

(1) Standing wave effect

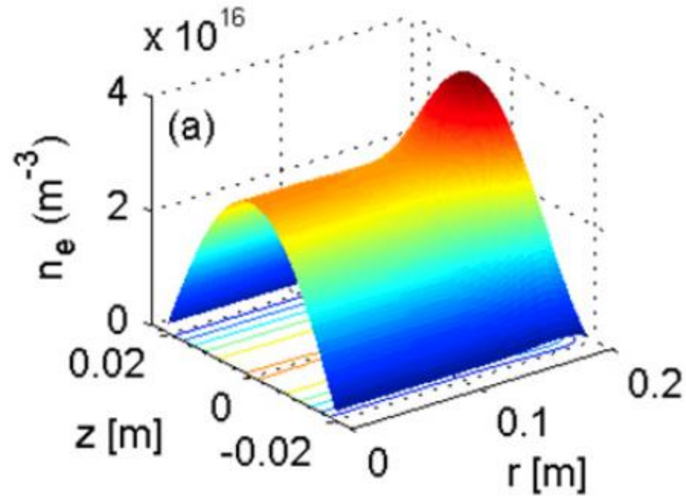

(2) Edge effects

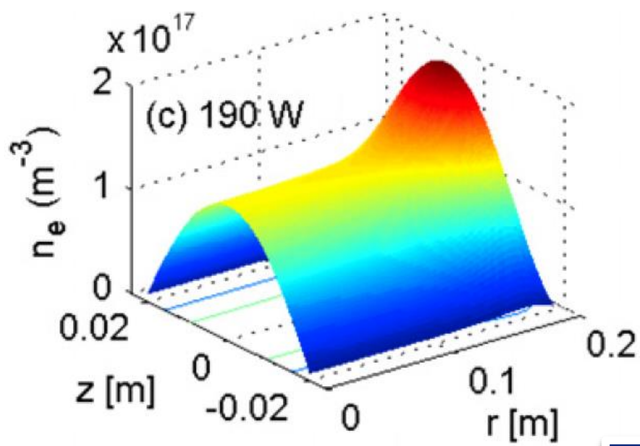

(3) Skin effect

- Lee I, Graves D B, Lieberman M A. *Plasma Sources Sci. Technol.*, 2008, 17(1): 015018.

1.1 Introduction: causes of plasma nonuniformity

➢ Two distinct electromagnetic modes

Even (symmetric) mode

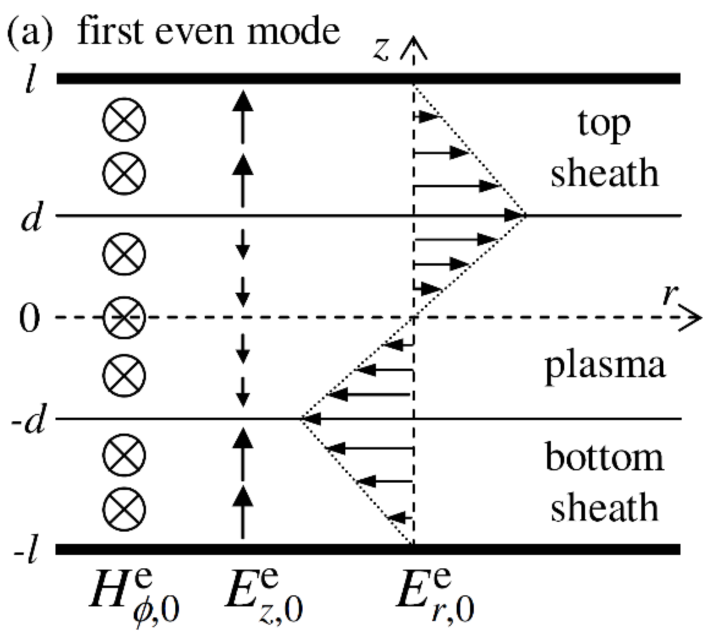

Standing wave effect

Odd (asymmetric) mode

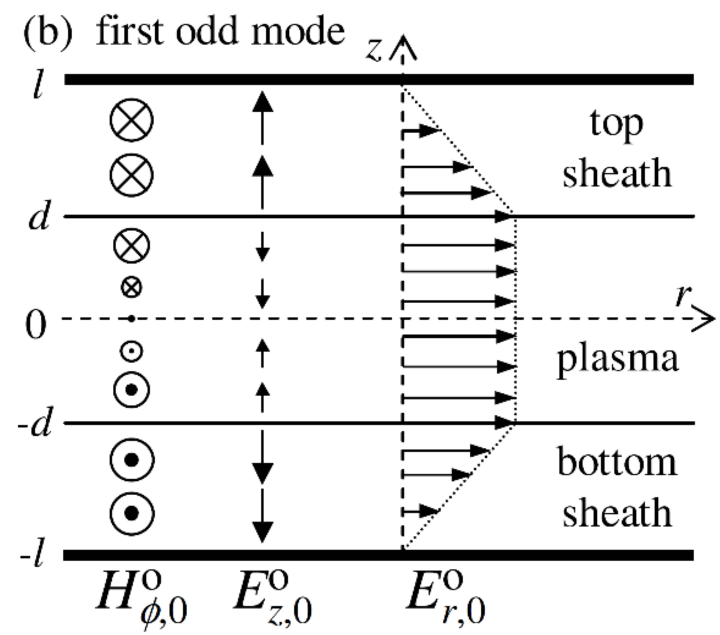

Telegraph effect

➢ Sansonnens L, Howling A A, Hollenstein C. *Plasma Sources Sci. Technol.*, 2006, 15(3): 302-313.

1.1 Introduction: standing wave effect

Previous studies

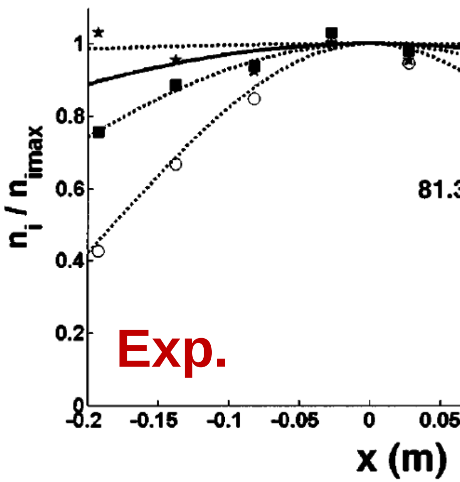

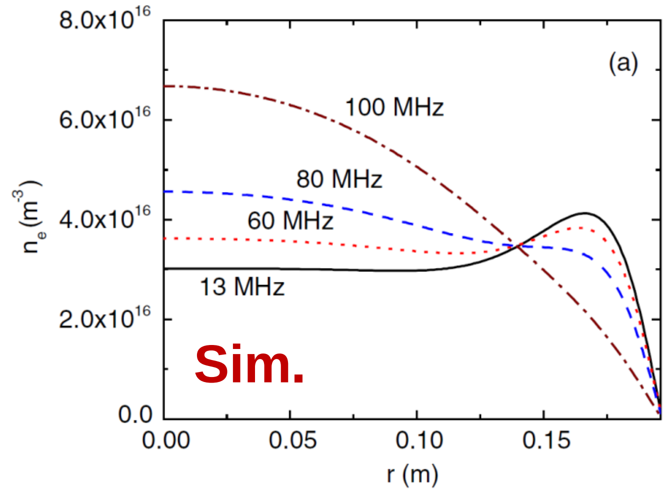

Our work

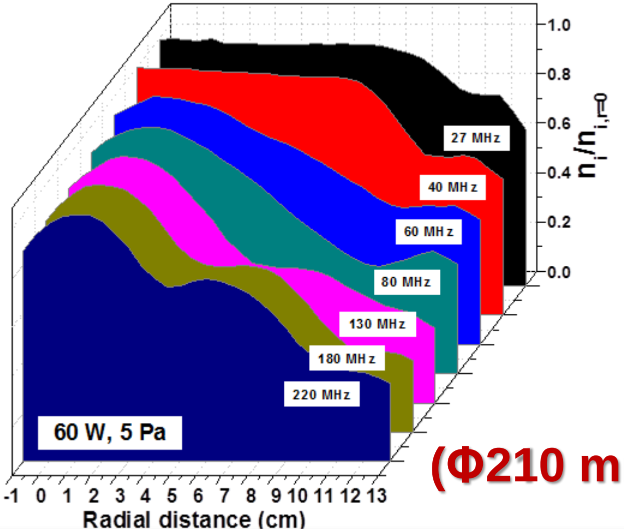

(Φ210 mm)

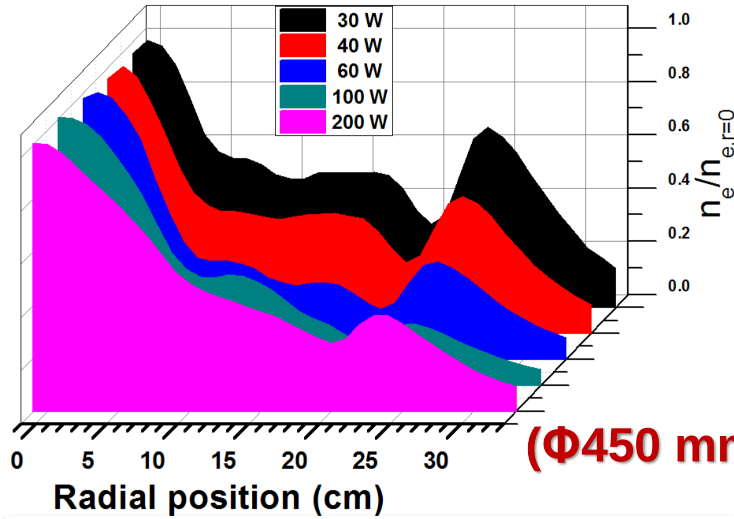

(Φ450 mm)

- Perret A, *et al. Appl. Phys. Lett.*, 2003, 83(2): 243-245.
- Lee I, *et al. Plasma Sources Sci. Technol.*, 2008, 17(1): 015018.
- Liu Y X, *et al. Plasma Sources Sci. Technol.*, (2015) 24, 025013.
- Liu Y X, *et al. J. Appl. Phys.*, (2014) 113, 043303.
- Han D M, *et al. J. Appl. Phys.*, (2016) 119, 113302.

1.1 Introduction: nonlinear standing wave excitation

- **Lieberman *et al.* developed a transmission line model, which predicted that the higher harmonics excited by PSR can lead to spatial resonances, significantly enhancing the power deposition at the reactor center.**

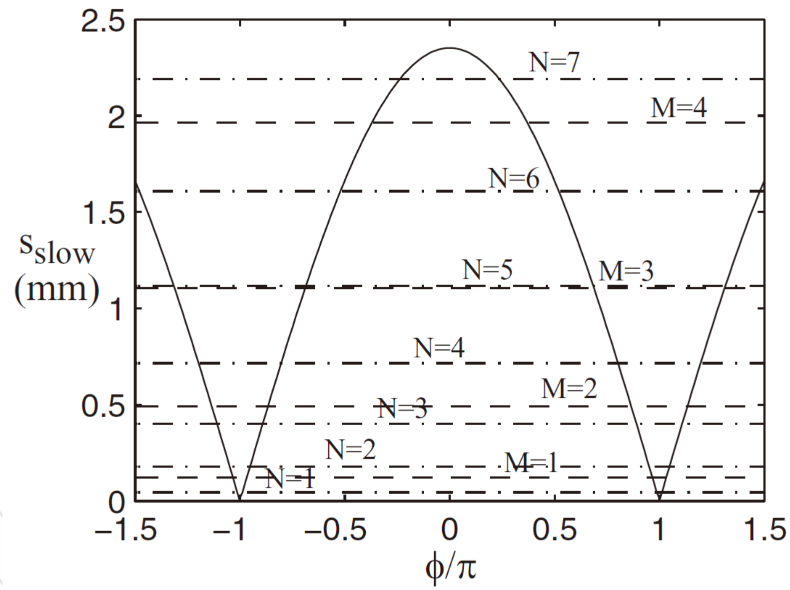

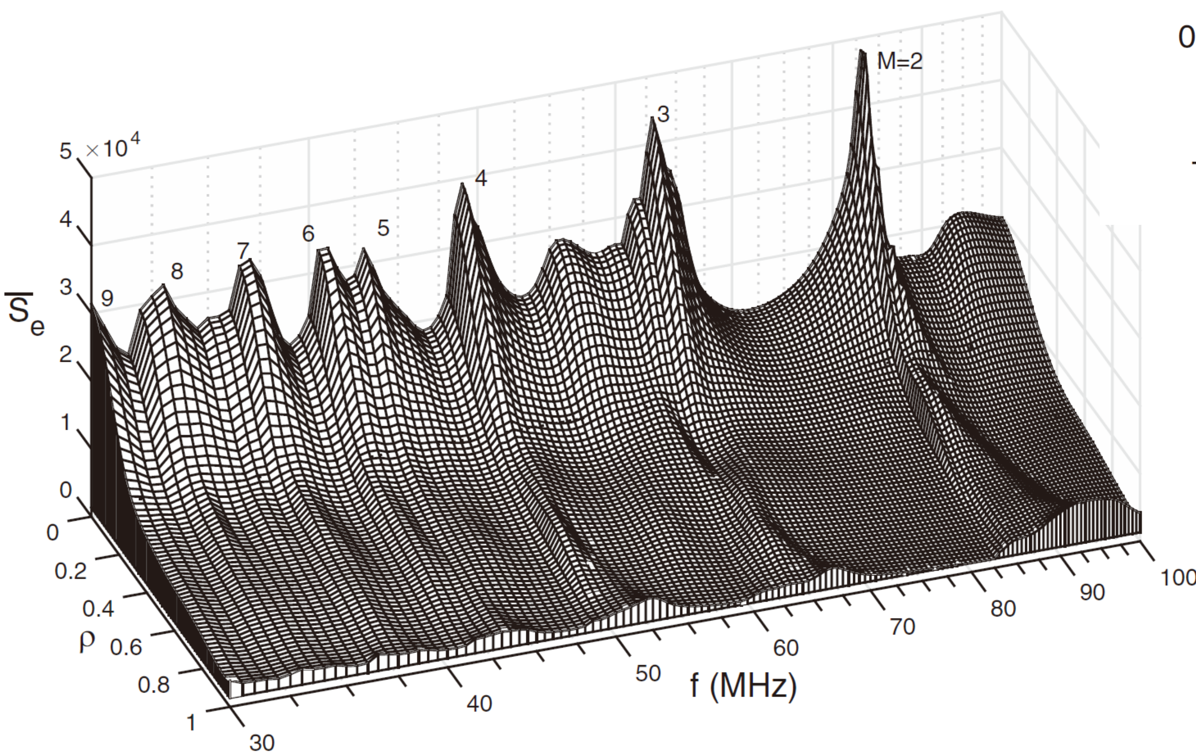

- **Lieberman M A, *et al. Plasma Sources Sci. Technol.*, 24, 055011 (2015).**
- **Wen D Q, *et al. Plasma Sources Sci. Technol.*, 26, 015007 (2016).**

1.2.1 Experimental setup and diagnostics

➢ Schematic diagram of CCP reactor

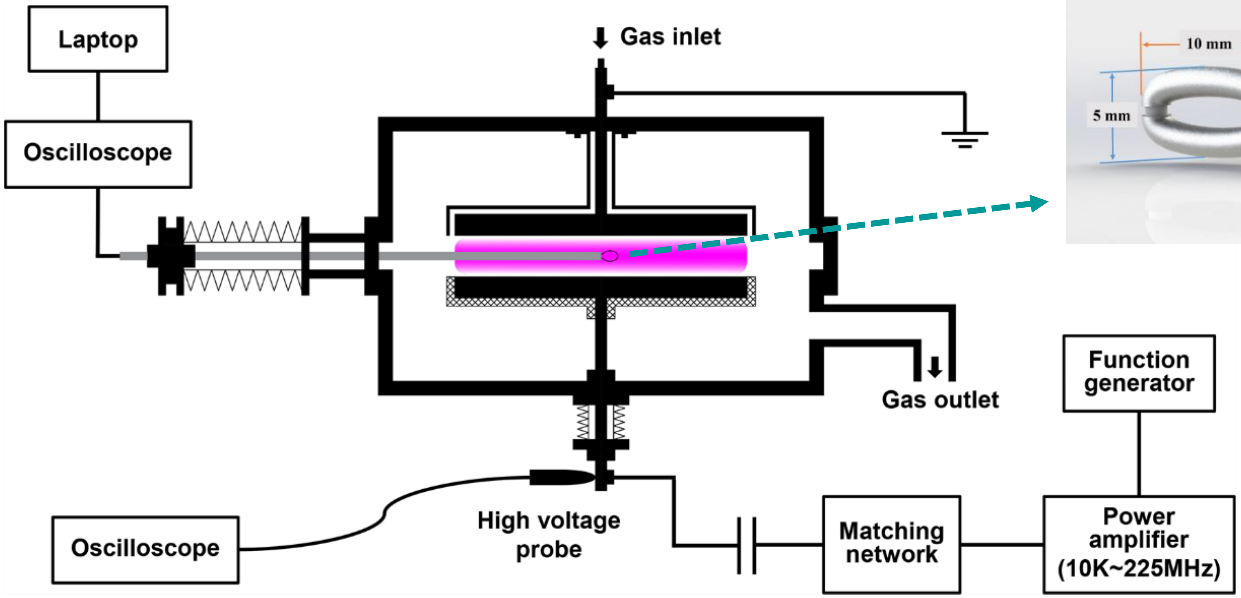

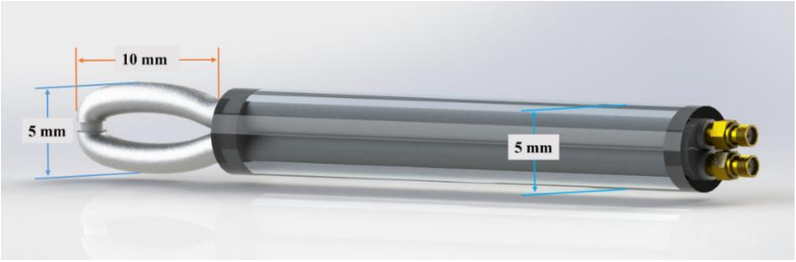

External parameter

Reactor diameter: 28 cm
Electrode diameter: 21 cm
Electrode gap: 3 cm

Working gas: argon
Pressure: 3 - 50 Pa
Flow rate: 40 SCCM

Driving frequency:
13.56/60/100 MHz

➢ Diagnostic methods

1) High-frequency, high-voltage probe
2) Floating double probe
3) High-frequency B-dot probe

1.2.2 Numerical model

> - Lieberman M A, *et al. Plasma Sources Sci. Technol.*, 24, 055011 (2015).
> - Zhao K, *et al. Physical review letters*, 2019, 122(18): 185002.

➢ Nonlinear transmission line model

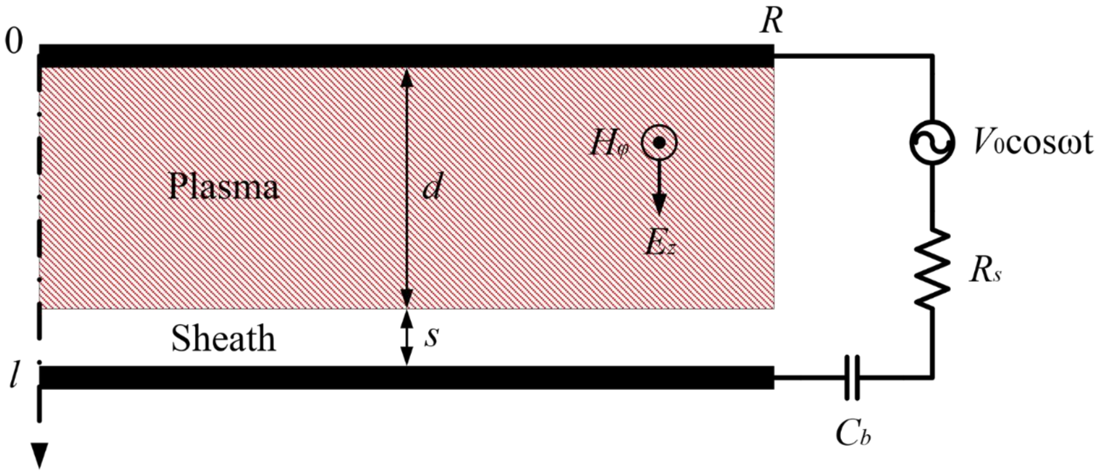

$$\begin{cases} \nabla \times \mathbf{H} = \mathbf{J} \\ \nabla \times \mathbf{E} = -\mu_0 \dfrac{\partial \mathbf{H}}{\partial t} \end{cases}$$

$$\frac{1}{r}\frac{\partial}{\partial r}\left(r\frac{\partial V}{\partial r}\right) = \mu_0 l \frac{\partial J}{\partial t}$$

$$\begin{cases} \dfrac{\partial \Sigma}{\partial t} = J - J_{i0} + J_{e0} e^{-V_s/T_e}, \Sigma > 0 \\ \dfrac{\partial J}{\partial t} = \dfrac{e^2 n_e}{md}(V + V_b - V_s) - \nu J \end{cases}$$

$$\begin{cases} \left.\dfrac{\partial V(r,t)}{\partial r}\right|_{r=0} = 0 \\ V(R,t) = V_0 \cos \omega t - I_R(t) R_s \end{cases}$$

$$V_s = 0.51 V_0 \frac{H^{1.159}}{h_l^{0.841}} \left(\frac{\Sigma}{\Sigma_0}\right)^{1.681} \left(\frac{T_e}{V_0}\right)^{0.159}$$

$$\left\langle \int_0^R 2\pi r dr J(r,t) \right\rangle_{\omega t} = 0$$

1.3 Results: a comparison between ES and EM cases

- **Spatial structure of the physical quantities (*n* = 1-5)**

13.56/60/100MHz, 80W, 3Pa

Harmonic magnetic field

Harmonic voltage

Harmonic current

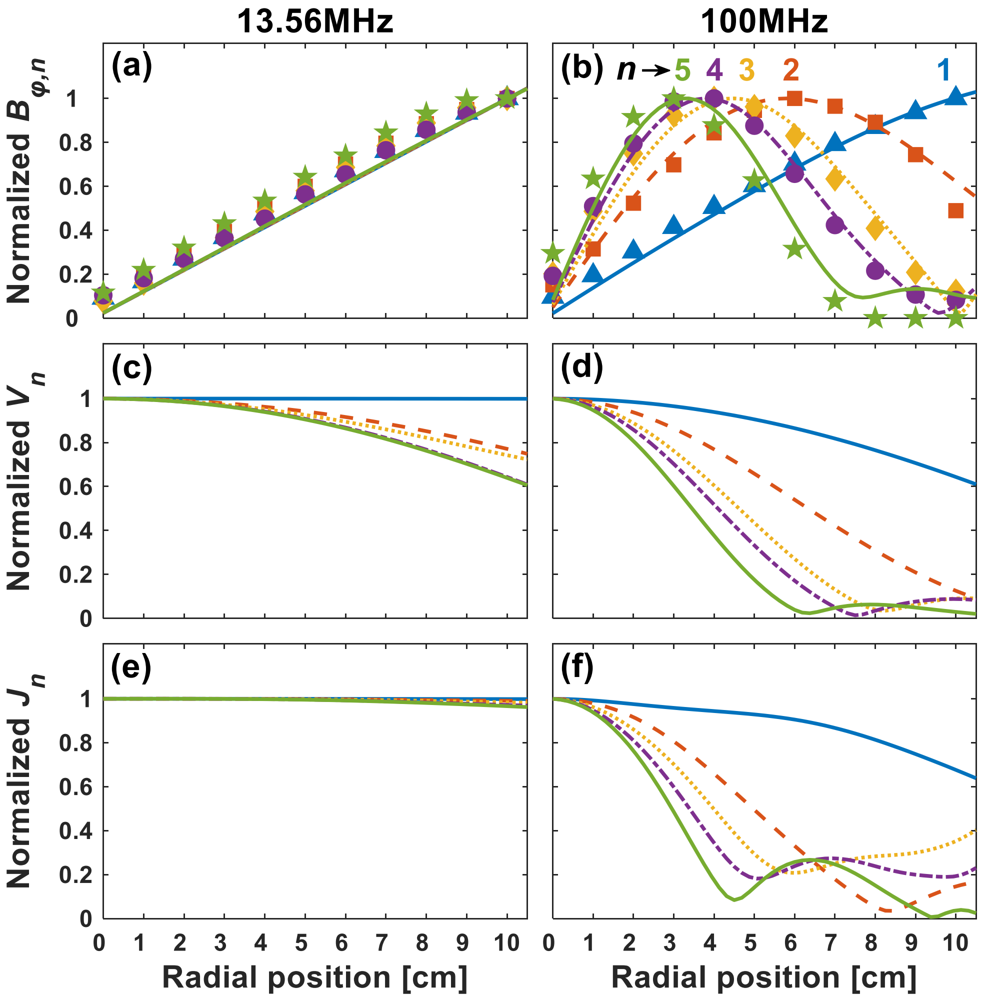

$$(1)\, J_n \propto \frac{dB_{\varphi,n}}{dr} \qquad (2)\, k_p R_1 = \chi_{01}$$

***R*₁**: distance from the node to the electrode center

***k*ₚ**: wave number of radially propagating surface waves

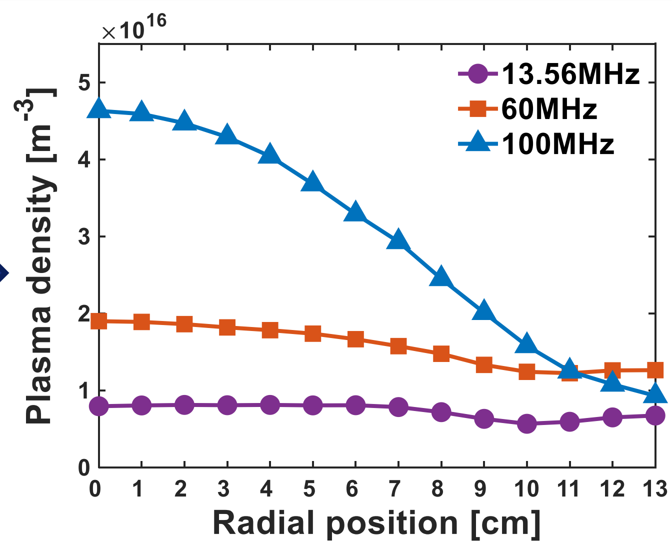

Plasma density

1.3 Results: a comparison between ES and EM cases

➢ **Spatiotemporal dynamics of the sheath**

13.56/100MHz, 80W, 3Pa

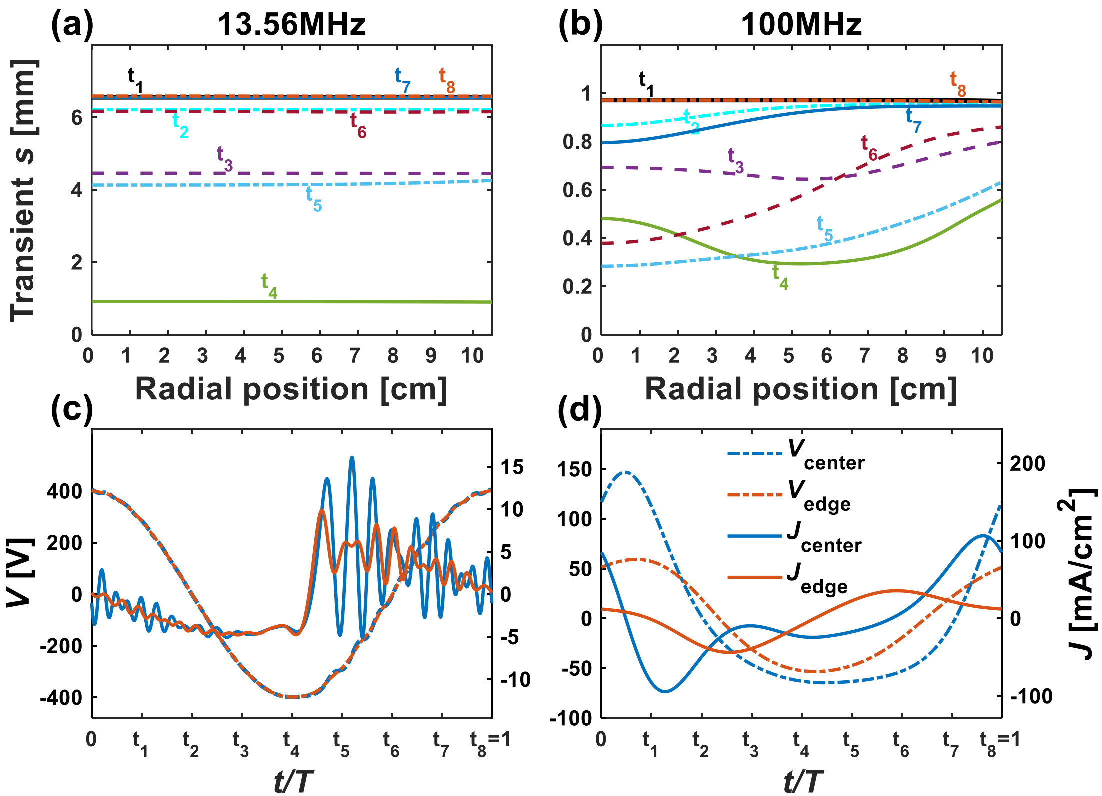

Sheath thickness versus radius in eight equally spaced times over one rf cycle

Waveforms of the total discharge voltage and current at the electrode center and edge

➢ **At 100 MHz: a higher voltage, a thinner sheath and a higher speed of sheath motion prevail at the center, contributing to a center-high plasma density.**

➢ Zhao K, *et al. Physical review letters*, 2019, 122(18): 185002.

1.3 Results: a comparison between ES and EM cases

13.56/100MHz, 80W, 3Pa

- **Coupling between plasma series resonance (PSR) and spatial wave resonance (SWR)**

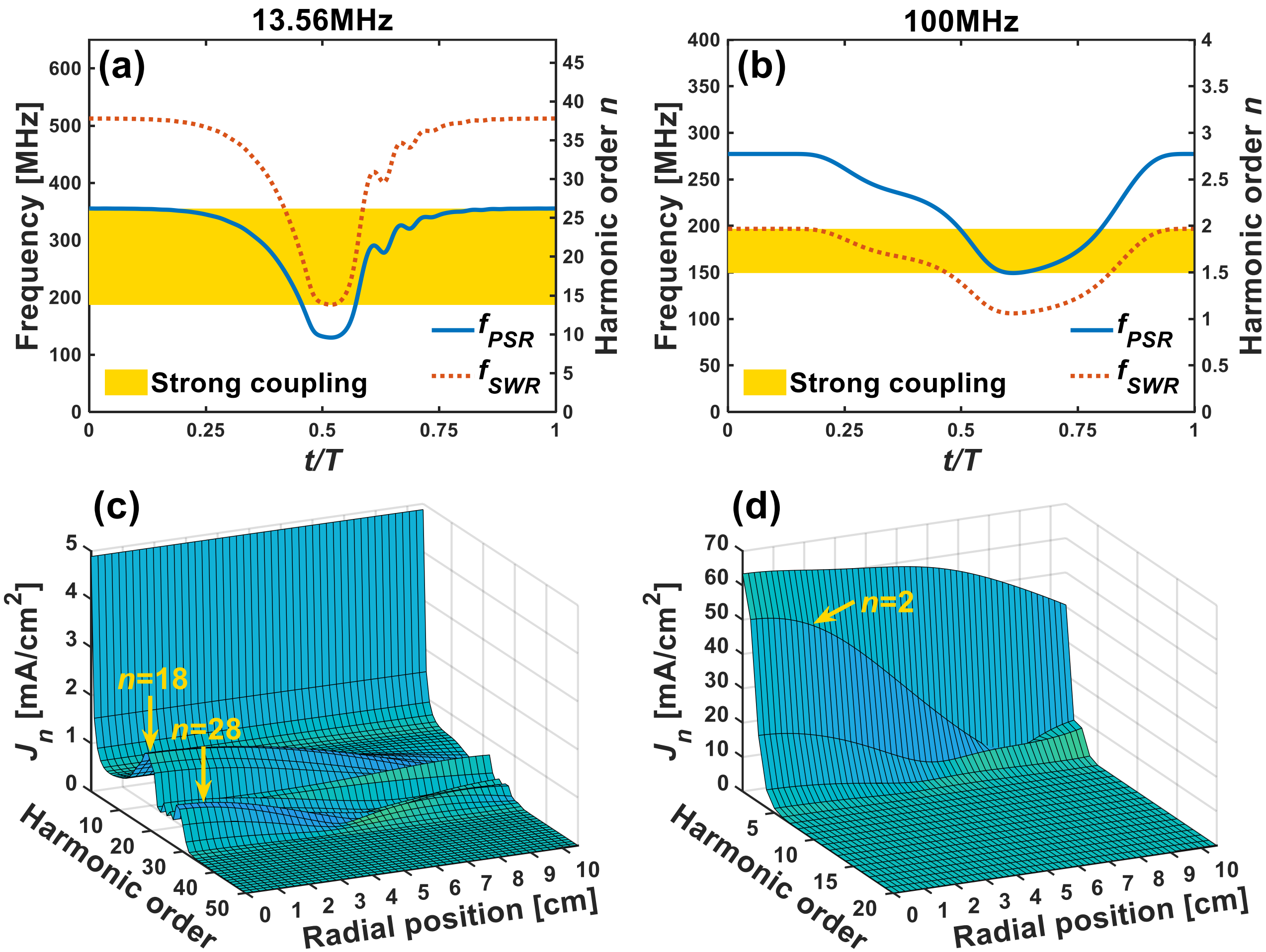

- **PSR frequency:**

$$\omega_{PSR}=\left(\frac{s}{l}\right)^{1/2}\omega_p=N\omega$$

- **SWR frequency**

$$\omega_{SWR}=\left(\frac{s}{l}\right)^{1/2}\frac{\chi_{0m}c}{R}=M\omega$$

- **A strong coupling occur at:** $N=M$

◆ **13.56 MHz：**

$$15<N=M<29$$

◆ **100 MHz：**

$$N=M=2$$

1.3 Results: effect of gas pressure on higher harmonics

100MHz, 80W, 3-50Pa

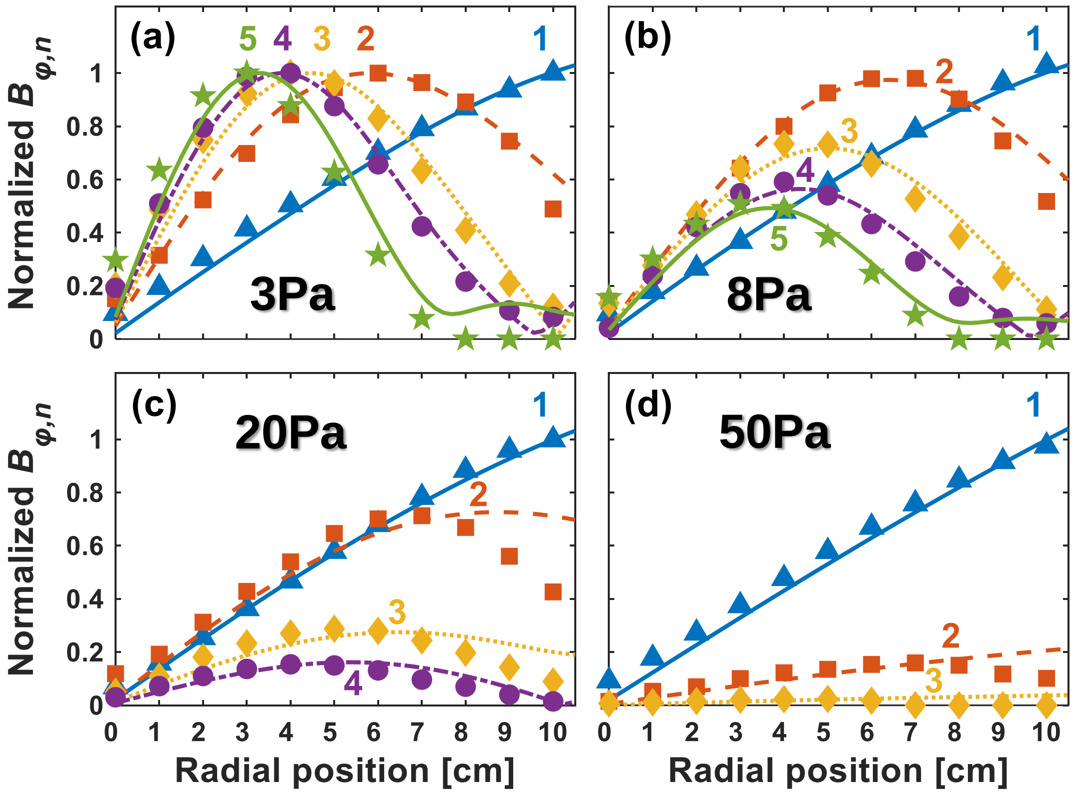

Harmonic magnetic field (*n*=1-5)

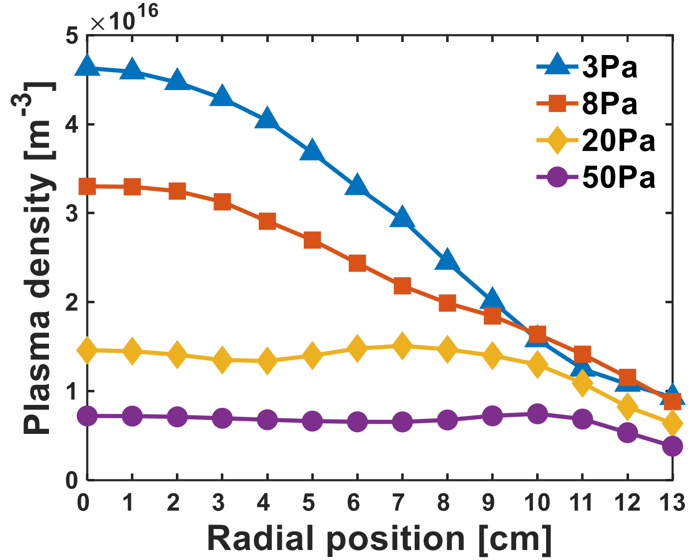

Plasma density

- **The higher harmonics decay dramatically with pressure, resulting in improved plasma uniformity.**

➢ Zhao K, *et al. Physical review letters*, 2019, 122(18): 185002.

2 Suppressing nonlinear standing wave excitation via the EAE

2.1 Introduction: PSR oscillations

➢ PSR oscillations in geometrically *asymmetric* discharges

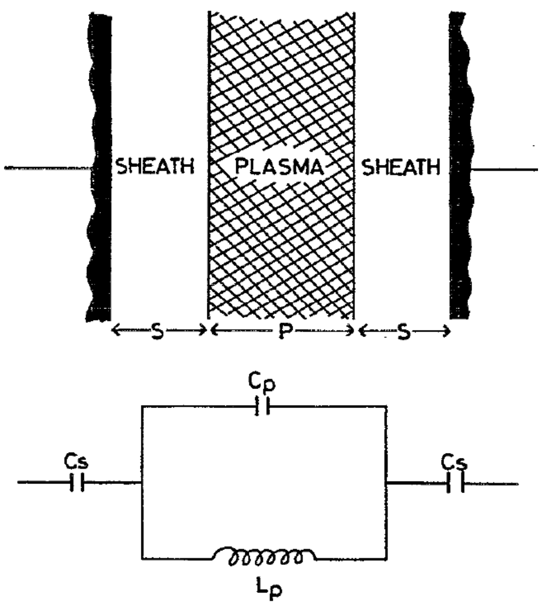

FIG. 1. Schematic diagram of the plasma model.

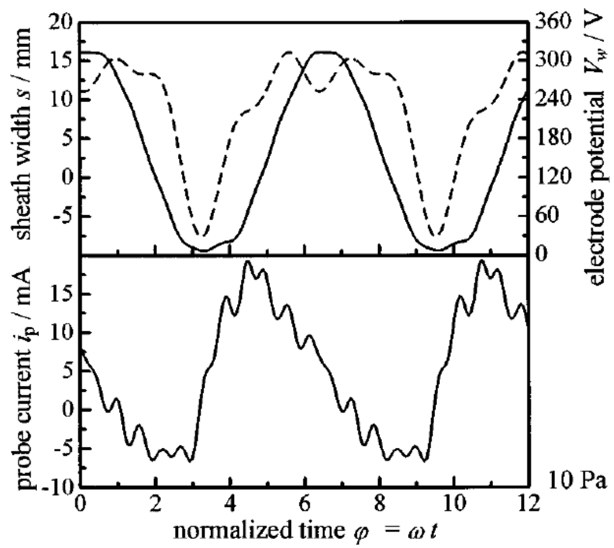

FIG. 6. Measured current in an asymmetrical Ar rf discharge. The solid and the dashed lines represent the probe current and the electrode potential respectively. Bias voltage U_B=153 V and rf amplitude $\hat{U}$=155 V.

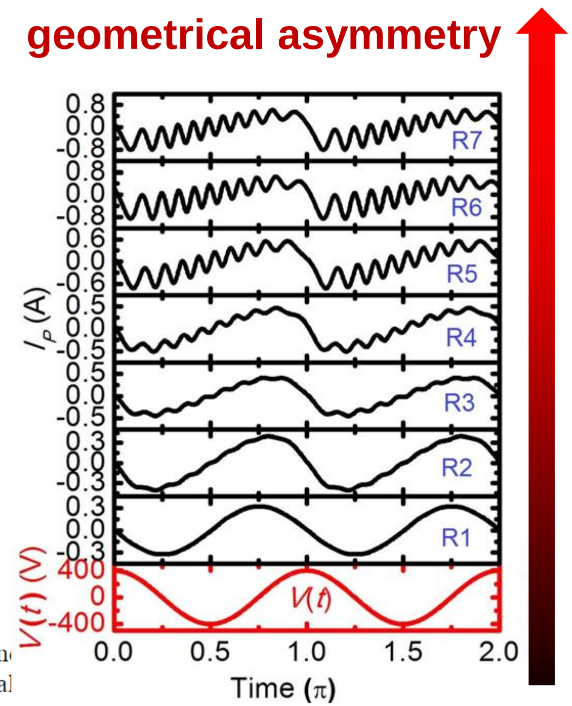

- ➢ Annaratone B M, Ku V P T, Allen J E. *Journal of Applied Physics*, 1995, 77(10): 5455-5457.
- ➢ Klick M. *Journal of applied physics*, 1996, 79(7): 3445-3452.
- ➢ Bora B, Soto L. *Physics of Plasmas*, 2014, 21(8): 083509.

2.1 Introduction: PSR oscillations & EAE

➢ **PSR oscillations in geometrically *symmetric* discharges**

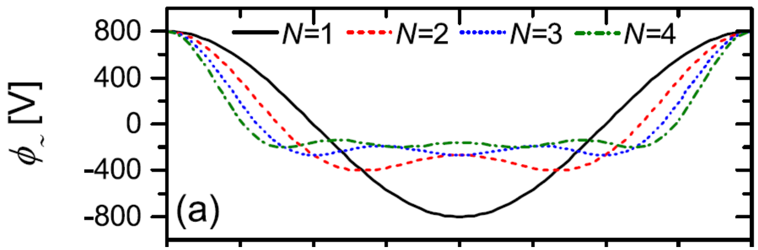

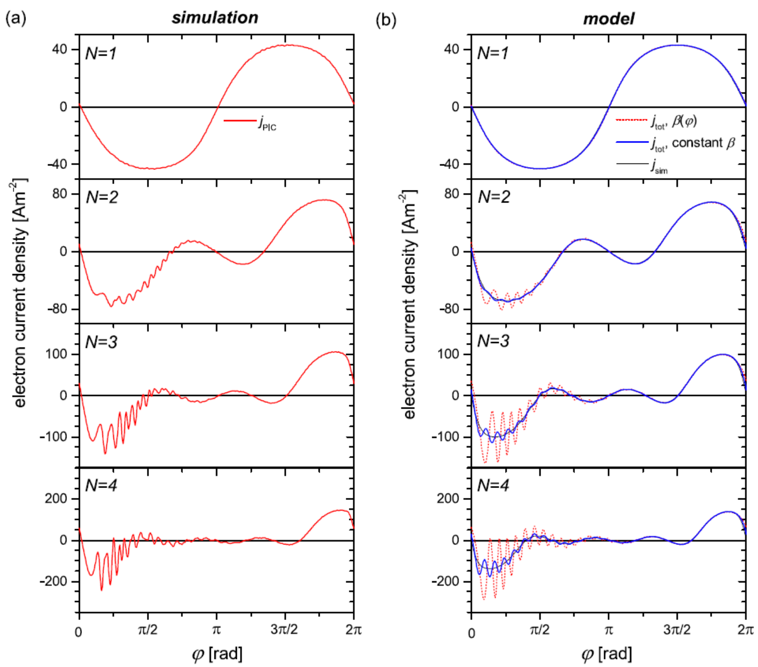

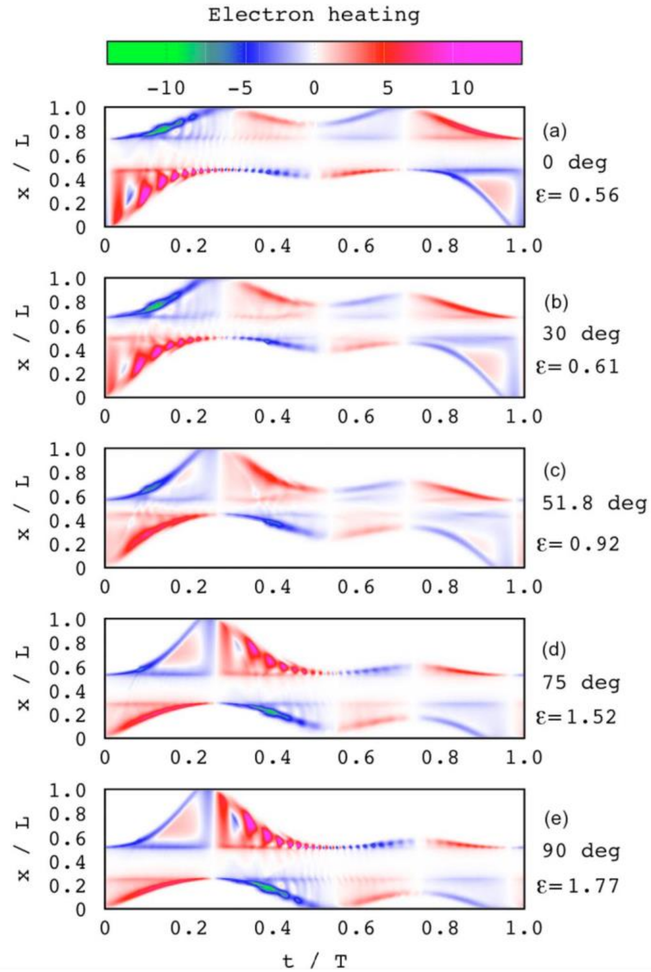

➢ Schüngel E, *et al. Plasma Sources Sci. Technol.*, 24, 044009 (2015).
➢ Donkó Z, *et al. Applied Physics Letters*, 2009, 94(13): 131501.

2.1 Introduction: PSR oscillations & EAE

➢ **PSR oscillations in a CCP with *finite electrode asymmetry***

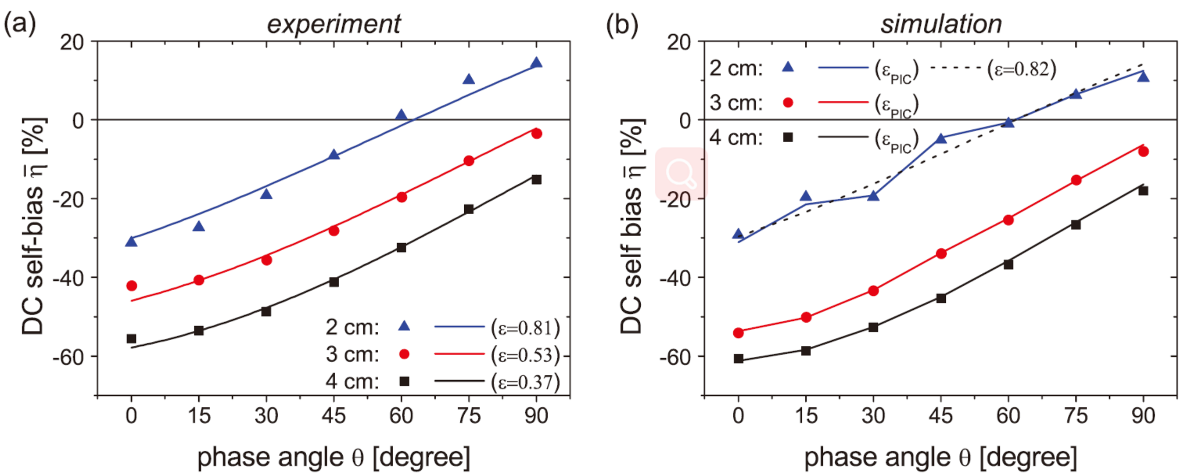

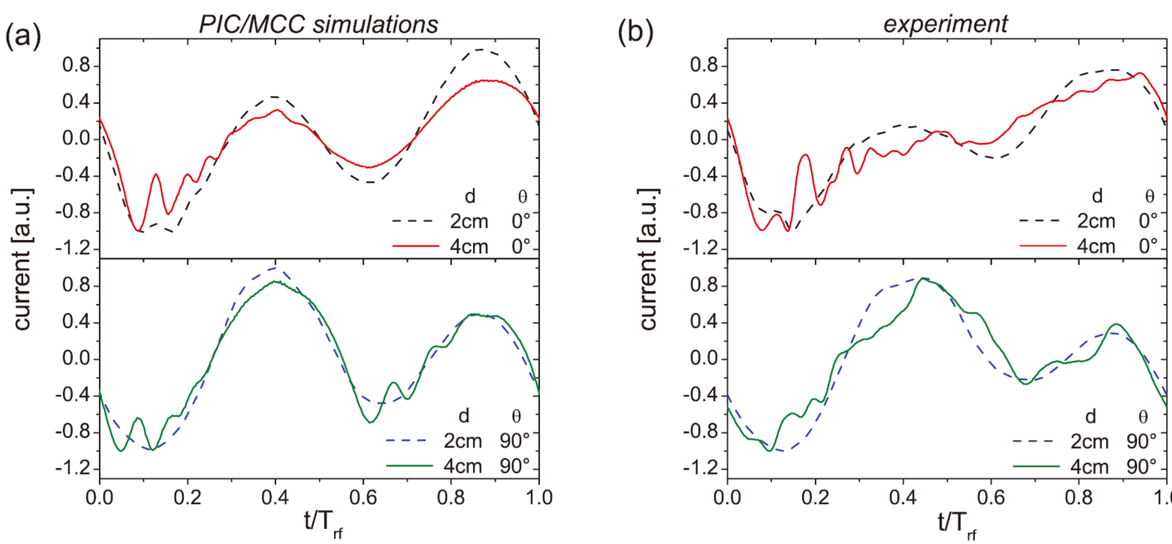

➢ Schüngel E, *et al. Journal of Applied Physics*, 2012, 112(5): 053302.

2.1 Introduction: PSR oscillations & EAE

➢ **Optimizing plasma uniformity via the *EAE***

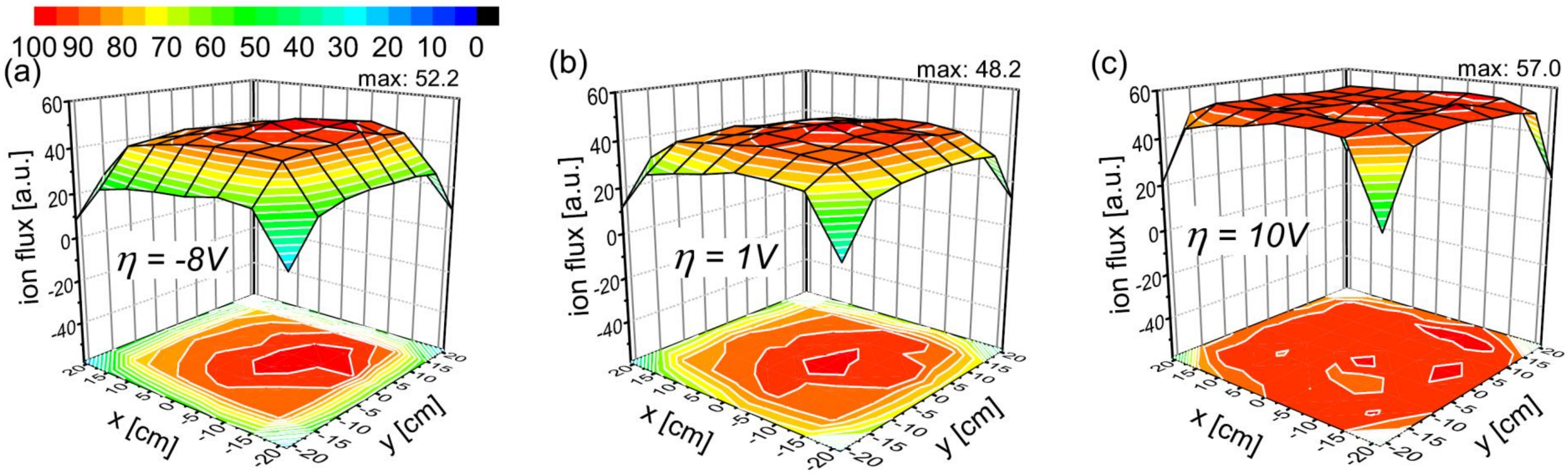

➢ **Lateral inhomogeneities of the plasma density caused by standing wave effects can be *eliminated* based on the *EAE*.**

➢ **Nevertheless, the important interaction of the nonlinear standing wave excitation with the plasma nonuniformities was *inevitably neglected*.**

➢ **Schüngel E, *et al*. *Applied Physics Letters*, 2015, 106(5): 054108.**

2.2 Experimental setup and diagnostics

➢ **Schematic diagram of CCP reactor**

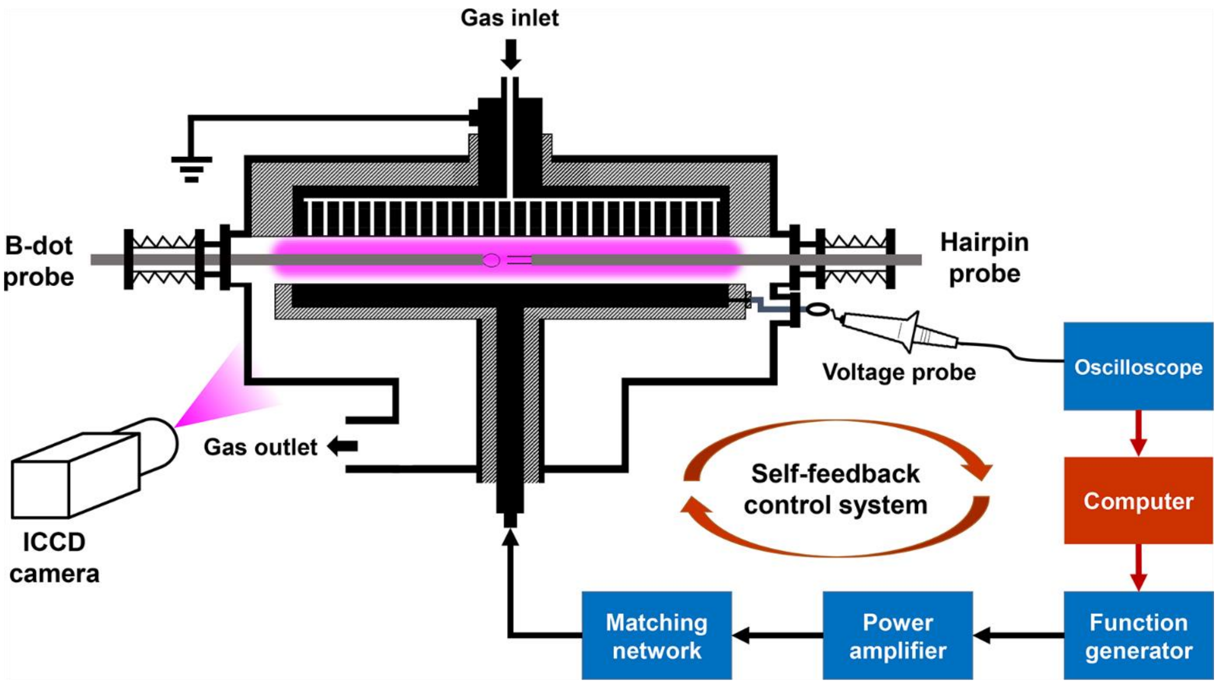

External parameter

Reactor diameter: 40 cm
Electrode diameter: 30 cm
Electrode gap: 4 cm

Working gas: argon
Pressure: 4 Pa
Flow rate: 40 SCCM

Driving frequencies:
30MHz & 60MHz

➢ **Diagnostic methods**

1) High-frequency, high-voltage probe
2) Resonance hairpin probe
3) High-frequency B-dot probe
4) ICCD camera

Target voltage waveform:

$$V_{rf}(t) = V_0[\cos(2\pi ft + \theta) + \cos(4\pi ft)]$$

$$V_0 = 30\mathrm{V},\ f = 30\mathrm{MHz}$$

2.3 Results: plasma density

DC self-bias

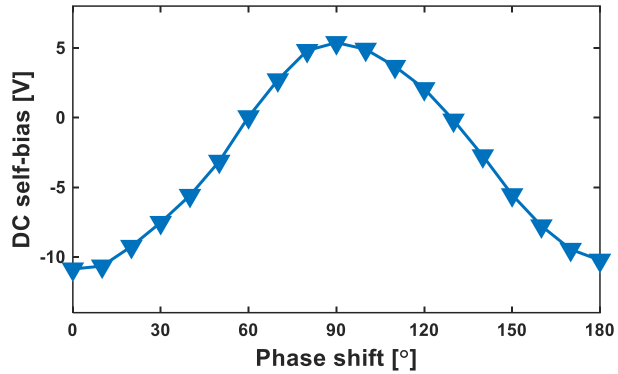

Plasma density at the reactor center

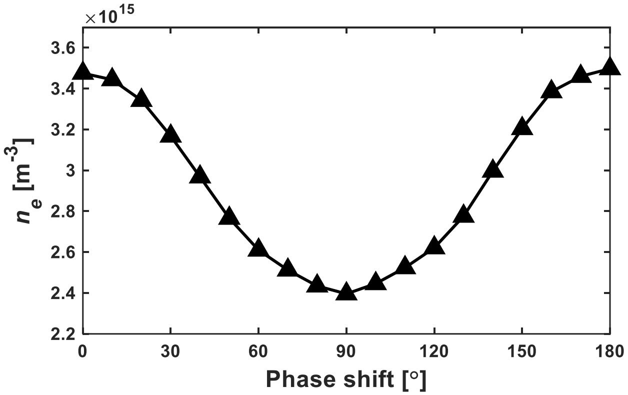

Axial distribution of the optical emission intensity

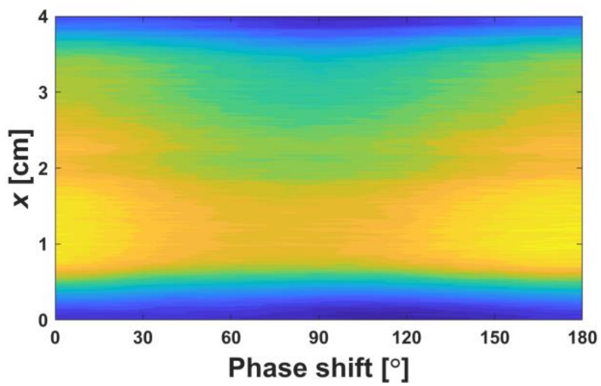

- A variation in the ***DC self-bias***, the ***central plasma density***, and the ***optical emission intensity*** with ***θ*** can be clearly identified.
- Nonlinear SWE becomes ***remarkable*** as DC self-bias reaches a ***minimum***.

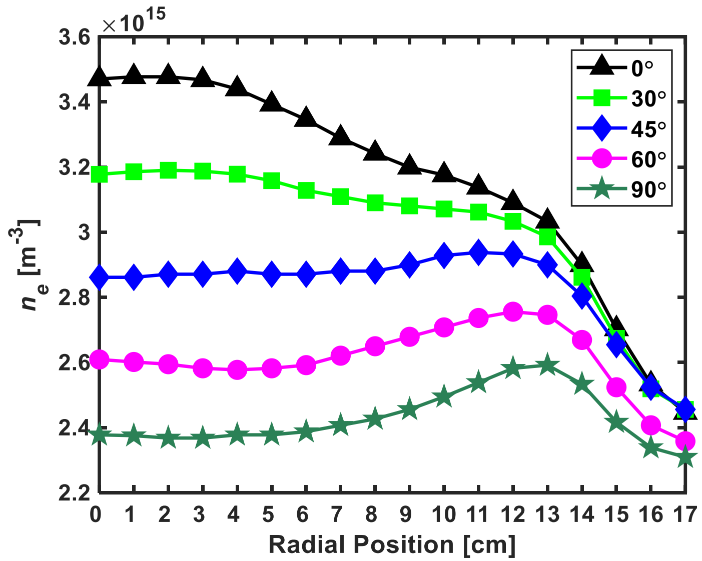

Radial distributions of the plasma density

➢ Zhao K, *et al. in preparation.*

2.3 Results: harmonic magnetic field

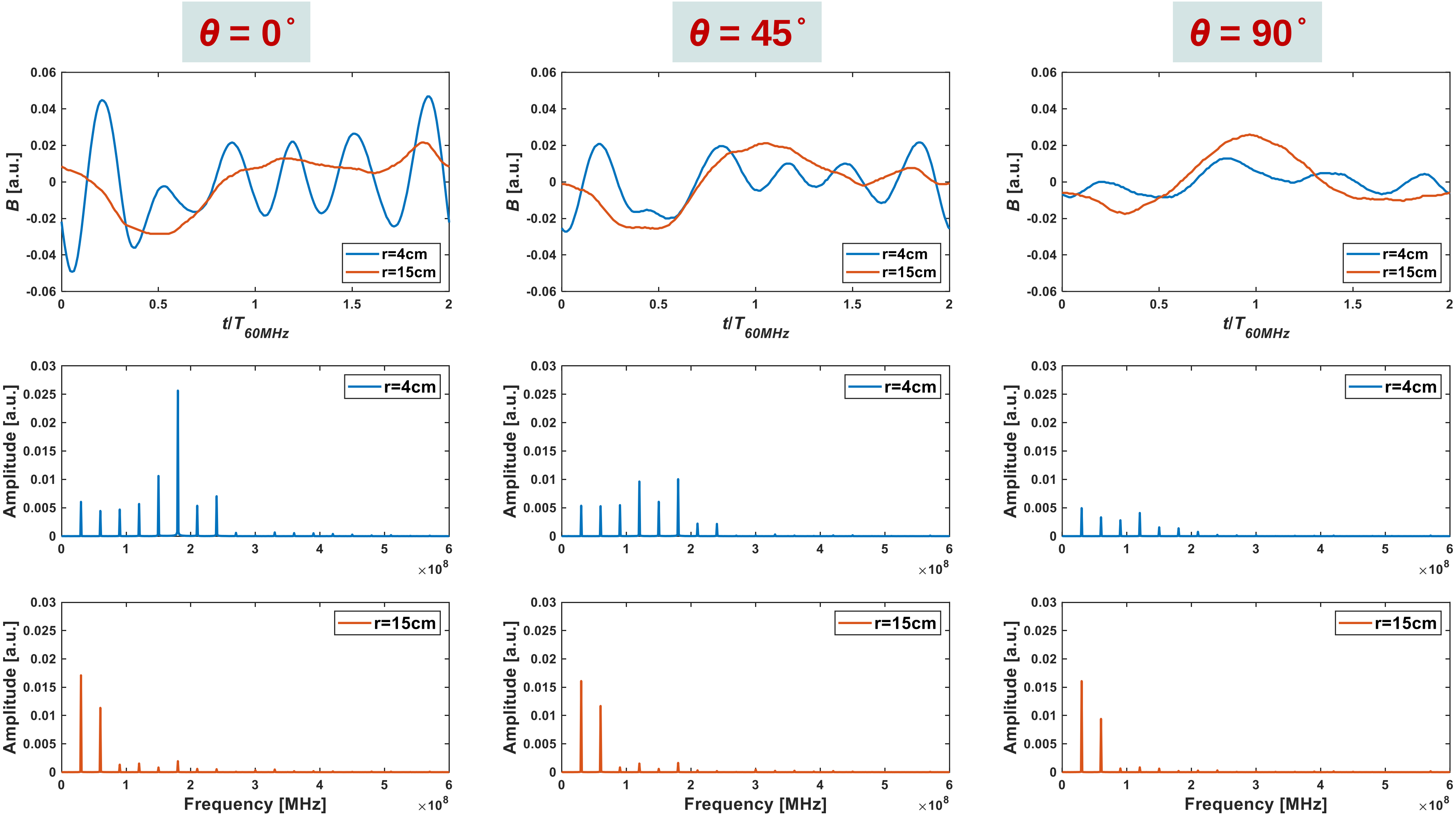

Raw signals from the B-dot probe for different θ

➢ Zhao K, *et al. in preparation.*

2.3 Results: harmonic magnetic field/current

Harmonic magnetic field

Harmonic current

***θ* = 0°**

***θ* = 45°**

***θ* = 90°**

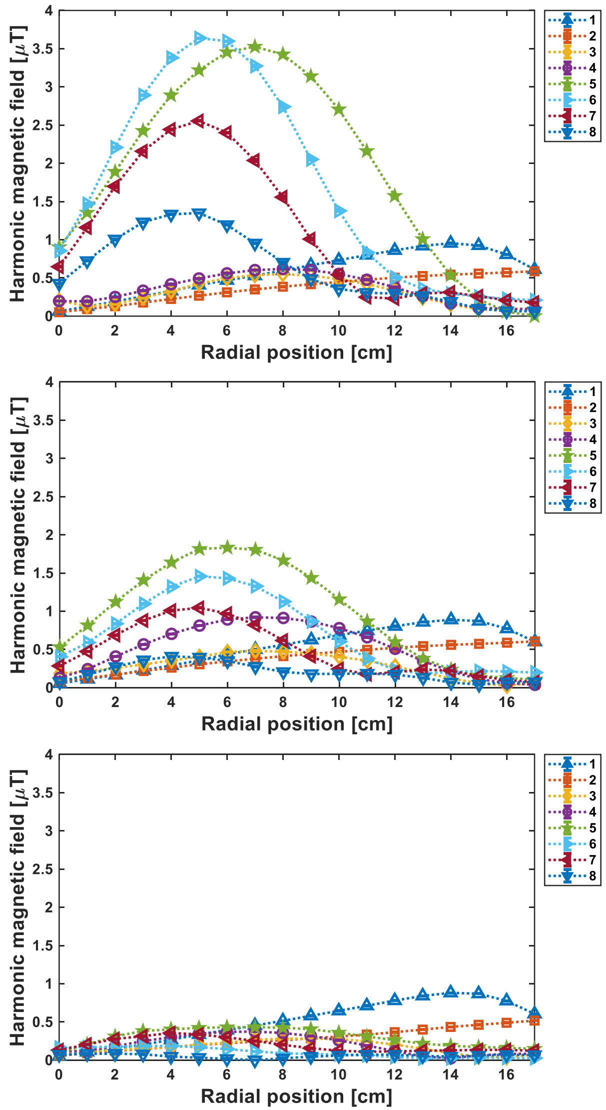

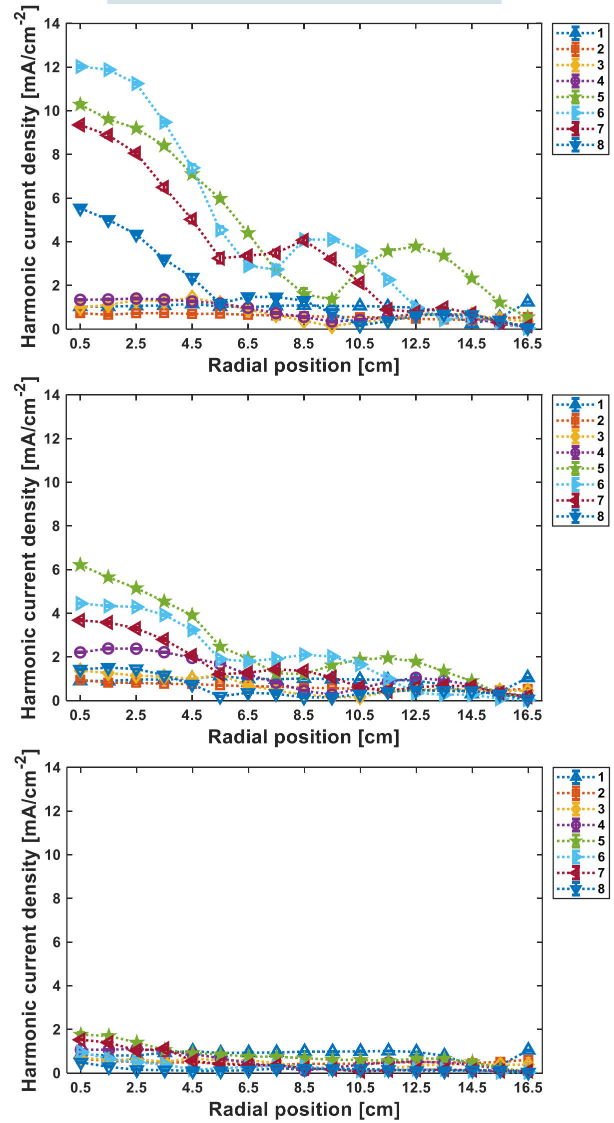

3 Role of the low-frequency source on the nonlinear standing wave excitation in a dual-frequency CCP

3.1 Introduction: ways to improve the plasma uniformity

A) Special-shape electrodes

B) Power source and external circuit
- **1. Phase shift control**
- **2. Electrical asymmetry effect**

◆ **Another way to suppress the SWE:**

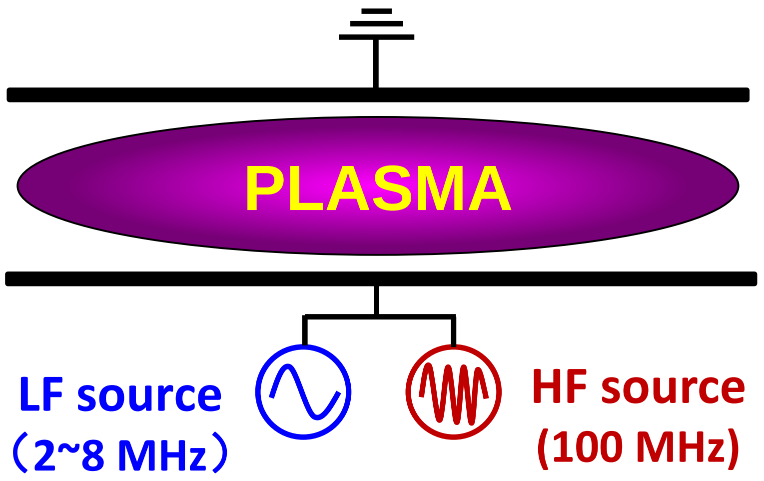

◆ **Advantages：**

1) By regulating the LF parameters, the plasma uniformity can be optimized;

2) The independent control of the ion flux and ion energy can be achieved.

3.2 Experimental setup and diagnostics

➢ **Schematic diagram of CCP reactor**

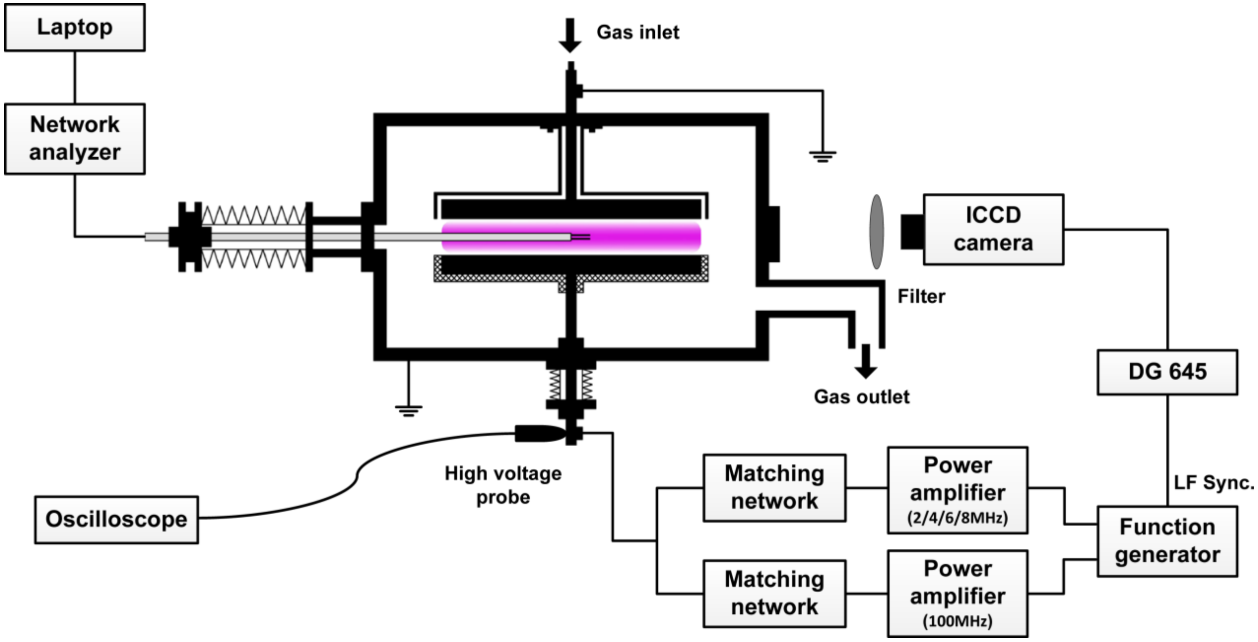

External parameter

Reactor diameter: 28 cm
Electrode diameter: 21 cm
Electrode gap: 3 cm

Working gas: argon
Pressure: 1-40Pa
Flow rate: 40 SCCM

Driving frequency:
HF+LF ➡ 100+4MHz

➢ **Diagnostic methods**

1) **Resonance hairpin probe**
2) **ICCD camera**
3) **High-frequency B-dot probe**

➢ Zhao K, *et al. Plasma Sources Sci. Technol.*, 2018, 27(5): 055017.

3.3 Results: effect of the LF voltage ϕ_L

➢ Sources parameters

HF : 100MHz @ 50V
LF : 4MHz @ 0/50/100/200/300V

Case I (8Pa)

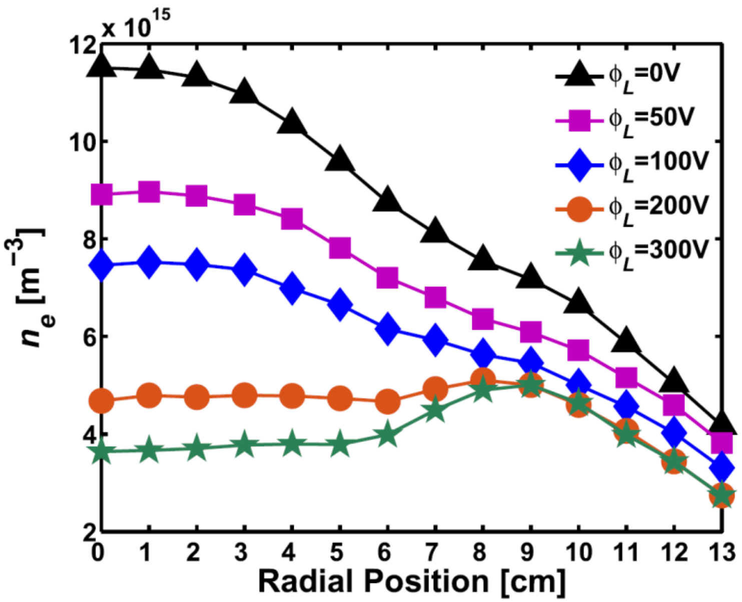

➢ Optimized LF voltage:
ϕ_L =200V !

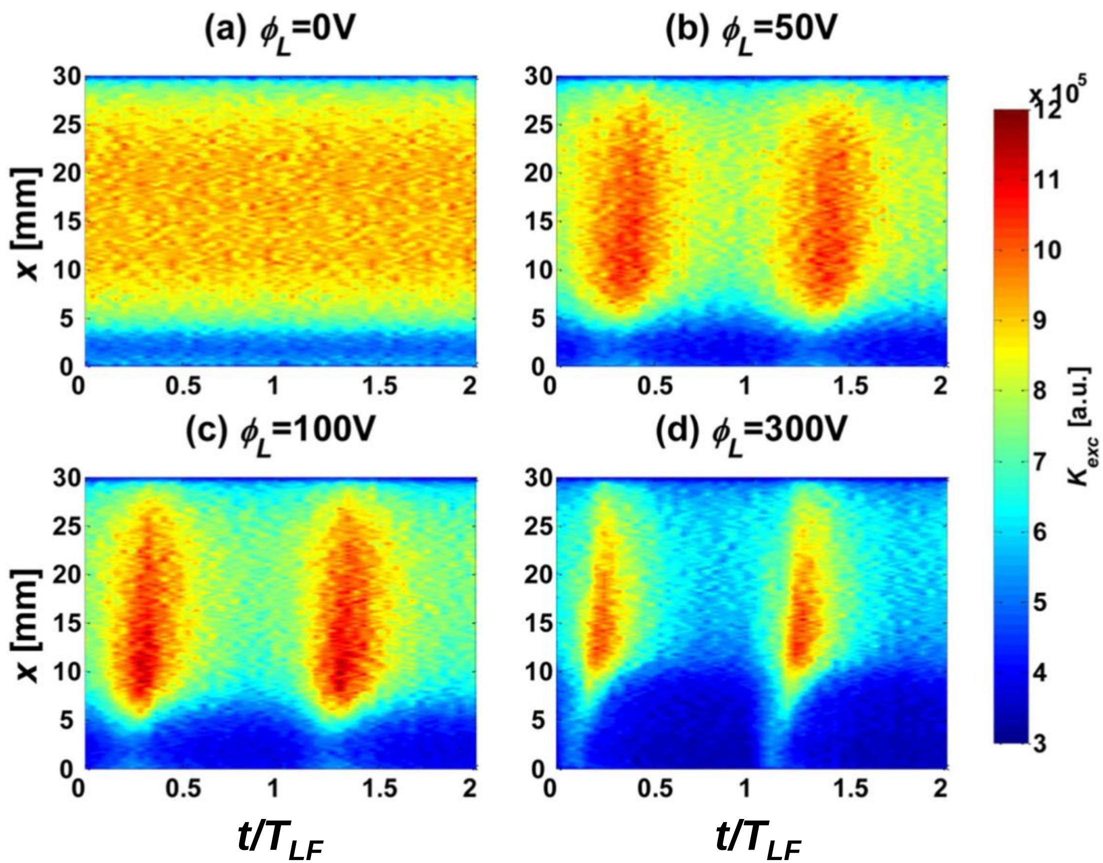

■ Spatiotemporal plots of the electron-impact excitation rate

➢ Zhao K, *et al. Plasma Sources Sci. Technol.*, 2018, 27(5): 055017.

3.3 Results: effect of the LF voltage ϕ_L

ϕ_L = 0V | ϕ_L = 50V

Electron-impact excitation rate

Magnetic field

FFT spectrum

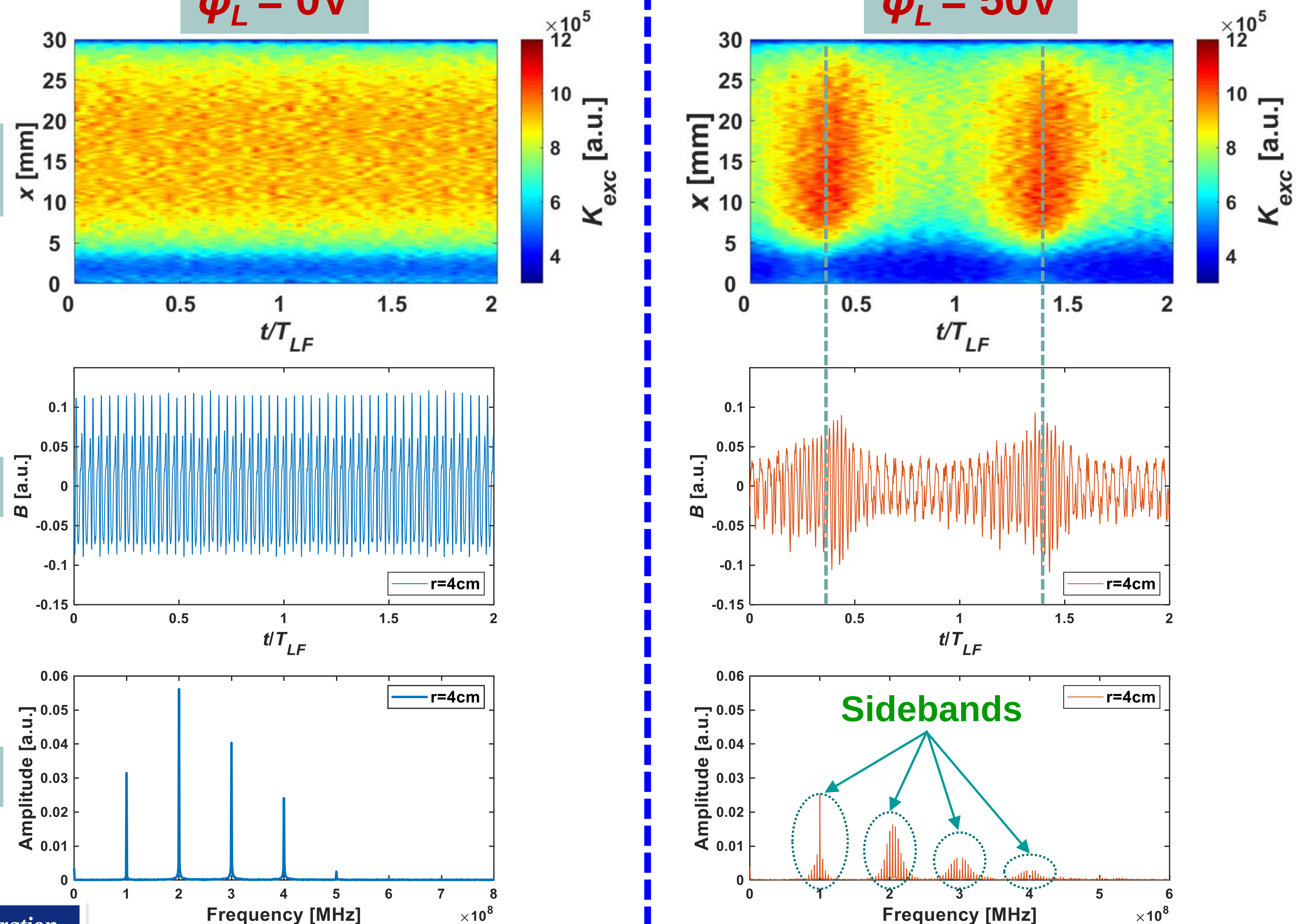

- Zhao K, *et al. in preparation.*

4 Summary

- **At relatively low pressure, higher harmonics enhanced by the nonlinear PSR can induce *radial standing waves*, with voltage and current *maxima on axis*, resulting in *center-high plasma density*.**

- **In an electrically asymmetric discharge driven by 30MHz and 60MHz, the nonlinear standing wave excitation can be *suppressed* by tuning the phase shift between the two driving frequencies, leading to an *improved plasma uniformity*.**

- **By introducing a second LF source into a VHF (100 MHz) capacitive discharge, the nonlinear standing wave excitation dominated by the HF source becomes *highly modulated* by the LF source, producing a series of *sidebands* of the harmonics.**

Acknowledge

- **This work is partially supported by the National Natural Science Foundation of China (NSFC).**
- **We also acknowledge Prof. Lieberman from University of California, Berkeley and Prof. Economou from University of Houston for their distinguished contribution to parts of this work.**

Thank You !

Appendix

Appendix-1

TABLE I. Radial maxima of the physical quantities for the first five harmonics in argon discharges driven at 13.56 and 100 MHz.

f [MHz]	13.56					100				
Harmonic order n	1	2	3	4	5	1	2	3	4	5
$B_{\varphi,n,\max}$ (Exp.) [μT]	3.2	0.9	0.5	0.2	0.2	22.8	16.4	-	-	-
$B_{\varphi,n,\max}$ (Sim.) [μT]	2.5	0.8	0.5	0.4	0.3	30.7	10.8	3.2	0.7	0.2
$V_{n,\max}$ (Sim.) [V]	400.8	0.8	0.5	0.5	0.6	94.1	37.6	11.2	3.0	0.7
$J_{n,\max}$ (Sim.) [mA/cm^2]	4.9	1.6	1.0	0.8	0.7	63.5	51.6	19.4	5.1	1.3

Appendix-2 Validation of the B-dot probe

➢ Output signals from the B-dot probe for three probe orientations

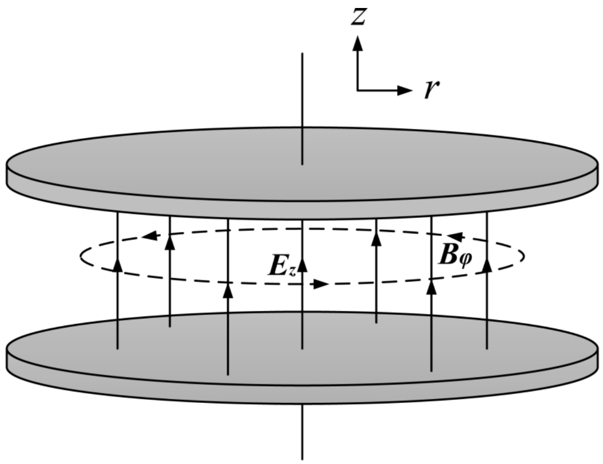

100MHz, 80W, 3Pa Radial position@4cm

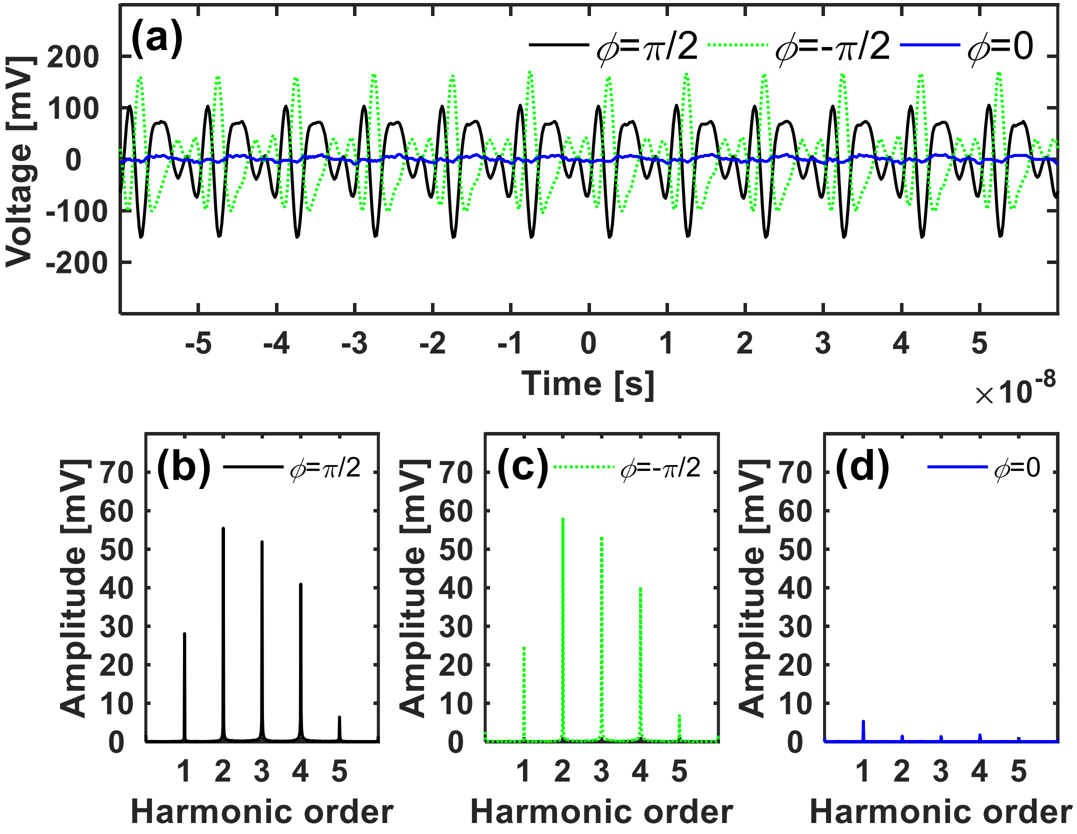

➢ Criteria to validate the B-dot probe measurements

1) $V_{\phi=0,n} \approx 0$

2) $V_{\phi=\pi/2,n} \approx V_{\phi=-\pi/2,n}$

■ $\phi = 0$: the plane of the probe coil is parallel to the electrodes